

Development and Characterization of Enteric-Coated Nanoparticles for Enhanced Oral Bioavailability of a BCS Class II Drug

Subhranshu Panda¹, Shubham Tikait^{2*}, Swati Deshmukh³

¹Director, School of Pharmaceutical Sciences, Jaipur National University (JNU), Jaipur, Rajasthan-302017, India

²Research Scholar, Jaipur National University (JNU), Jaipur, Rajasthan-302017, India

³Principal, Shraddha Institute of pharmacy (SIOPs), Washim, Maharashtra-444505, India

Received: 19th Oct, 2024; Revised: 9th Nov, 2024; Accepted: 25th Nov, 2024; Available Online: 25th Dec, 2024

ABSTRACT

Objective: The aim of the present study was to formulate and evaluate Rifaximin-loaded Eudragit-coated solid lipid nanoparticles (RFN-EC-SLN) to enhance oral bioavailability, provide sustained drug release, and improve therapeutic efficacy in treating gastrointestinal infections.

Methods: SLN were prepared using glyceryl monostearate (GMS) as lipid, Pluronic F68 as surfactant, and coated with Eudragit L100 polymer. The formulation was optimized using a BBD under QbD principles. Compatibility between drug and excipients was confirmed through FTIR and DSC. Surface morphology and particle structure were examined using SEM and TEM. *In-vitro* drug release and *ex-vivo* permeation was studied.

Results: FTIR and DSC analyses indicated no significant chemical interactions, confirming drug-excipient compatibility. SEM and TEM images revealed spherical nanoparticles with an diameter of ~160 nm, showing uniform dispersion and no aggregation. *In vitro* drug release demonstrated sustained release over 24 hours.

Conclusion: The developed RFN-EC-SLN formulation successfully improved the solubility, permeability, and sustained release profile of Rifaximin. The nanosystem offers a promising oral drug delivery approach for effective treatment of intestinal infections.

Keywords: Rifaximin, Solid Lipid Nanoparticles, Transmission Electron Microscopy, Box-Behnken Design, Sustained Release, P-gp Efflux Inhibition, Gastrointestinal Therapy, Quality by Design.

How to cite this article: Subhranshu Panda, Shubham Tikait, Swati Deshmukh. Development and Characterization of Enteric-Coated Nanoparticles for Enhanced Oral Bioavailability of a BCS Class II Drug. International Journal of Pharmaceutical Quality Assurance. 2024;15(4):2841-48. doi: 10.25258/ijpqa.15.4.95

Source of support: Nil.

Conflict of interest: None

INTRODUCTION

Oral administration remains the greatest ideal route for drug delivery due to its easiness of use, safety, and affordability. However, drugs classified under BCS Class II often exhibit poor aqueous solubility, which restricts absorption and reduces therapeutic effectiveness. Rifaximin, a poorly water-soluble antibiotic with minimal systemic absorption, is a typical example, as it mainly acts locally in the gastrointestinal tract but faces challenges related to solubility and release¹.

Advances in nanotechnology have introduced solid lipid nanoparticles (SLNs) as an auspicious strategy to address such limitations. SLNs, prepared using biocompatible lipids and stabilizers, offer developed solubility, stability, controlled release, and site-specific delivery. For lipophilic drugs like rifaximin, SLNs enhance dispersion in gastrointestinal fluids, thereby supporting better therapeutic outcomes².

Nevertheless, the oral administration of nanoparticles encounters barriers within the acidic gastric environment, which can cause drug degradation or premature release³. To mitigate these drawbacks, enteric coating technologies utilizing pH-responsive polymers such as Eudragit® L100 have gained prominence³. This coating remains stable

under gastric acidic conditions but dissolves at intestinal pH, ensuring targeted release while minimizing gastric irritation. Additionally, excipients such as Glyceryl Monostearate (as a lipid matrix) and Pluronic F68 (as a stabilizing surfactant) further contribute to the stability, dispersibility, and efficiency of the formulation^{4,5}.

The present work focuses on developing and optimizing enteric-coated SLNs of rifaximin to enhance solubility. The formulations were systematically evaluated for key parameters such as particle size, zeta potential, entrapment efficiency, drug loading, *in-vitro* release, and enteric protection, aiming to provide an effective delivery platform for poorly soluble drugs.

MATERIALS AND METHODS

Rifaximin as a gift sample from Cipla Pharmaceuticals Ltd., Mumbai. Glyceryl monostearate (GMS) and Eudragit L100 were procured from Loba Chemie and Evonik India Pvt. Ltd., respectively. Pluronic F68 was sourced from Sigma-Aldrich, USA. All solvents and reagents used in this research purchased from Merck Mumbai.

Preformulation Studies

Determination of Maximum Wavelength (λ_{max})⁶

*Author for Correspondence: shubhamtikait004@gmail.com

Table 1: Optimization of Rifaximin-loaded enteric-coated solid lipid nanoparticles (RFN-EC-SLN) formulation

Formulation	Drug	Formulation factors			Responses		
		Conc. of Lipid (mg)	Conc. of Surfactant (mg)	Conc. polymer (mg)	Particle size (nm)	Entrapment efficiency (%)	Drug release (%)
F1	20	50	600	60	152	72	84
F2	20	50	200	60	192	67	75
F3	20	50	400	80	182	75	78
F4	20	50	400	40	174	66	87
F5	20	100	200	40	168	74	82
F6	20	100	600	40	154	82	86
F7	20	100	600	80	185	82	75
F8	20	100	400	60	205	73	78
F9	20	100	200	80	210	77	69
F10	20	150	200	60	351	71	72
F11	20	150	600	60	248	80	74
F12	20	150	400	80	319	78	69
F13	20	150	400	40	295	76	76

A stock solution of Rifaximin was prepared by dissolving a deliberated quantity in methanol to obtain a conc. of 100 $\mu\text{g/mL}$. This solution was then diluted to 10 $\mu\text{g/mL}$ for UV-Visible spectrophotometric analysis. The sample was scanned over a wavelength range of 300 to 600 nm using methanol as the blank. The wavelength showing maximum absorbance was identified and recorded as the λ_{max} for Rifaximin.

Preparation of Calibration Curve⁷

A calibration curve was constructed using standard solutions of Rifaximin in methanol at conc. of 2, 4, 6, 8, and 10 $\mu\text{g/mL}$. The abs. of each solution was measured at the previously determined λ_{max} . A plot of absorbance

(AU) versus concentration ($\mu\text{g/mL}$) was generated, and a linear regression equation was calculated to determine the correlation coefficient (R^2) and assess the linearity of the method.

FTIR Spectroscopy⁸

FTIR spectroscopy was directed to investigate potential interactions between Rifaximin and formulation excipients. Samples of pure Rifaximin were prepared by triturating with potassium bromide (KBr) in a 1:100 ratio. The resulting pellets were scanned using an FTIR spectrophotometer (e.g., Bruker or PerkinElmer) in the range of 4000–400 cm^{-1} .

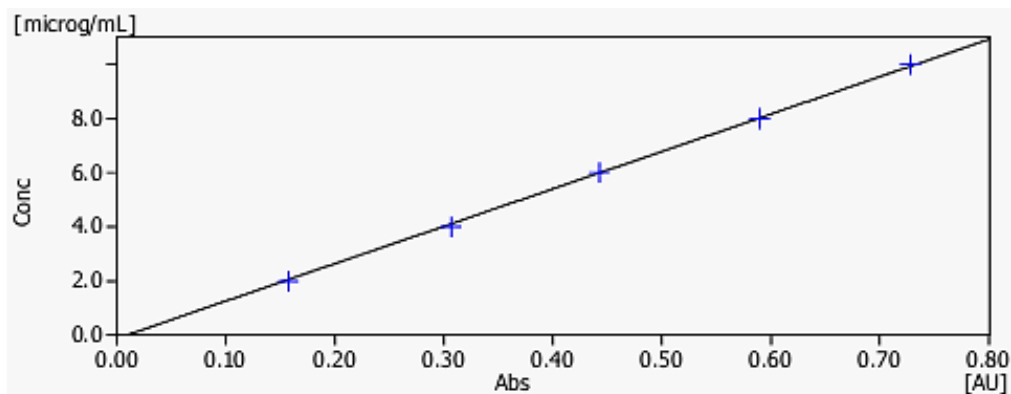


Figure 1: Calibration curve of Rifaximin in methanol (Absorbance vs. Concentration)

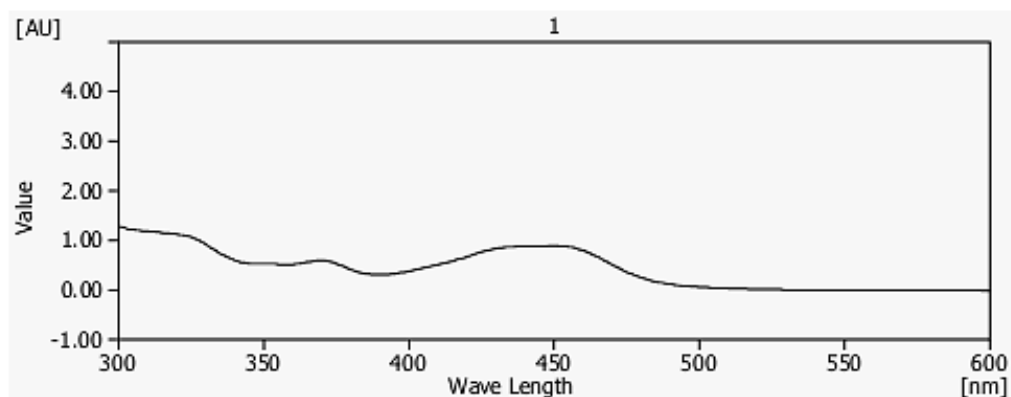


Figure 2: UV spectrum of Rifaximin showing peak absorbance around 337 nm

DSC Study⁹

DSC analysis was employed to assess thermal behaviour and drug-excipient compatibility. Approximately 2–5 mg of Rifaximin were weighed accurately and sealed in standard aluminum pans. The samples were heated from 30°C - 300°C at a rate of 10°C/min under a constant nitrogen purge. The thermograms were recorded using a calibrated DSC instrument (DSC 4000, PerkinElmer).

Preparation of Rifaximin-Loaded Enteric-Coated Solid Lipid Nanoparticles (RFN-EC-SLN)¹⁰⁻¹²

RFN-EC-SLN was prepared using the solvent injection method. Glyceryl monostearate (lipid phase) was dissolved in 5 mL of ethanol and melted in a water bath. Rifaximin (20 mg) was added to the molten lipid and sonicated for 1 minute using a probe sonicator (Qsonica Q500, USA). The aqueous phase (10 mL) containing Pluronic F68 was homogenized at 3000 rpm for 1 hour, into which the lipid solution was slowly injected. The resulting dispersion was ultracentrifuged at 10,000 rpm for 30 minutes to collect lipid aggregates. These aggregates

Table 2: Independent Variables levels used in BBD for RFN-EC-SLN optimization

Independent Variables	Level used, actual coded		
	Low (-1)	Medium (0)	High (+1)
A= Lipid: Glyceryl monostearate (mg)	50	100	150
B= Surfactant: Pluronic F68 (mg)	200	400	600
C= Polymer: Eudragit L100 (mg)	40	60	80

were re-dispersed in 10 mL of aqueous polyvinyl alcohol solution and stirred at 1000 rpm for 3 hrs. to form a uniform precipitate. For enteric coating, the precipitate was suspended in 10 mL of Eudragit L100 buffer (pH 6.8) and agitated at 1000 rpm for 2 hours, followed by probe sonication for 10 minutes. The final suspension formulation was centrifuged at 10 thousand rpm for 30 min. and freeze-dried to obtain RFN-EC-SLN.

Design and Optimization of RFN-EC-SLN using Box-

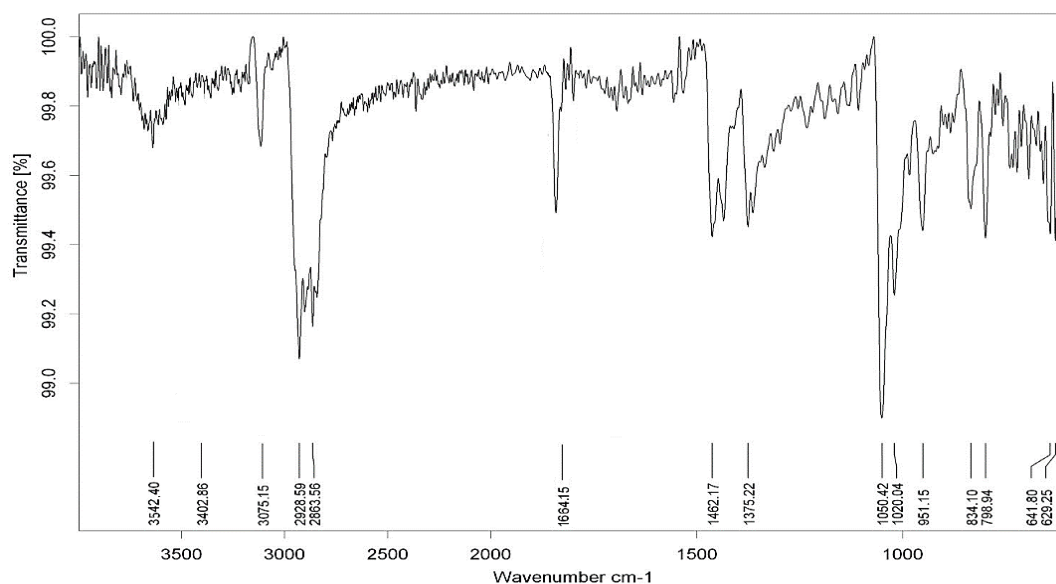


Figure 3: FTIR Spectra of Rifaximin

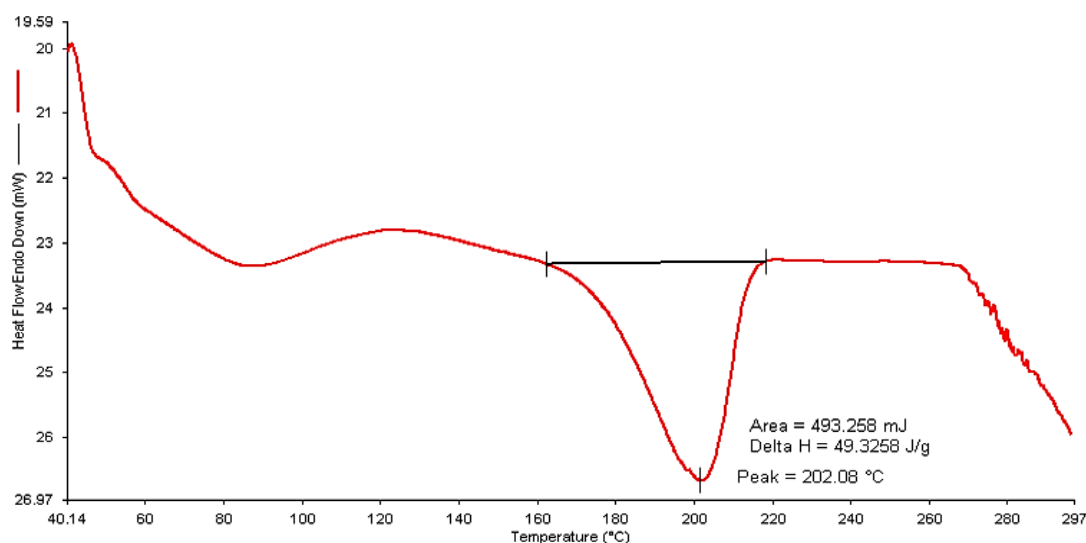


Figure 4: DSC thermogram of pure drug Rifaximin

Box-Behnken Design (BBD)¹¹⁻¹³

The preparation of rifaximin-loaded enteric-coated solid lipid nanoparticles (RFN-EC-SLN) was carried out through a Quality by Design (QbD)-guided strategy employing the BBD statistical model, executed using Design Expert software (version 13.0, Stat-Ease, USA). Three independent formulation variables-lipid concentration (factor A), surfactant concentration (factor B), and polymer amount (factor C) were investigated at three coded levels (-1, 0, +1). The dependent outcome variables selected for optimization were particle size (response Y1), entrapment efficiency (response Y2), and percentage drug release (response Y3).

Characterization RFN-EC-SLN Formulation**Particle Size, PDI, and Zeta Potential Analysis**¹⁴

The average particle size, size distribution (PDI), & zeta potential of RFN-EC-SLN formulation were analyzed (Zetasizer Nano ZS). PDI values indicated the uniformity of the nanoparticles, while zeta potential measurements served as predictors of colloidal stability based on electrostatic repulsion.

Entrapment Efficiency and Drug Content¹⁵

Encapsulation efficiency was determined by centrifuging 1 mL of the nanoparticle suspension (1 mg/mL drug) at 15,000×g for 30 min. at 4 °C. The supernatant was diluted with methanol, and the drug content was quantified using UV-Visible spectrophotometry at 296 nm.

pH Measurement¹⁶

The pH of the optimized formulation was determined at 37 °C using a calibrated digital pH meter (Ohaus ST10 Pen Meter).

For direct measurement, the electrode was carefully immersed into the nanoparticle dispersion, ensuring values reflected physiologically relevant conditions.

Scanning Electron Microscopy (SEM)¹⁷

The external morphology of RFN-EC-SLN was visualized using SEM (JEOL JMS-7400, Japan). A drop of the sample was applied to a silicon wafer, dried at 25 °C, and observed under high-resolution imaging to assess shape and surface characteristics.

Transmission Electron Microscopy (TEM)¹⁸

TEM analysis (JEOL 1230, USA) was performed to examine the internal structure and nanocarrier shape. Diluted RFN-EC-SLN was dropped onto 300-mesh copper grids, dried, and visualized under high magnification for structural evaluation.

In-vitro Drug Release Study¹⁹

Drug release from the optimized RFN-EC-SLN was studied using dialysis cassettes (MWCO 2,000 Da). The formulation was exposed to simulated gastric fluid (pH 1.2) for 2 hours, followed by transfer to simulated intestinal fluid (pH 6.8) for 22 hours. Samples collected at intervals were analyzed by UV spectrophotometry to calculate cumulative release.

Stability Studies^{20,21}

Accelerated stability testing was performed as per ICH Q1A(R2) guidelines in a chamber set at 40 ± 2 °C/75 ± 5% RH for three months. Formulations were periodically evaluated for drug content, particle size, PDI, zeta

potential, and physical appearance to confirm stability under stress conditions.

Statistical Analysis²²

Each experiment was performed in triplicate, and the findings are expressed as mean values with their corresponding standard deviations. Data interpretation and statistical validation were carried out using GraphPad Prism software (version 10.0).

RESULT AND DISCUSSIONS**Maximum Wavelength Detection**

The UV-Visible spectrophotometric analysis of Rifaximin revealed that the drug exhibited its maximum absorbance at 337 nm. This wavelength corresponds to the point of highest absorption in the scanned range, making it the most suitable for quantitative estimation. The λ_{max} was determined by scanning a diluted solution of Rifaximin between 300 to 600 nm using methanol as a blank. (Figure 1 & 2)

Calibration Curve of Rifaximin

The calibration curve for Rifaximin was constructed using standard solutions ranging from 2 to 10 µg/mL in methanol. Absorbance values were recorded at 337 nm. A linear regression analysis was performed, yielding the equation:

$$\text{Absorbance} = 0.0742 \times \text{Concentration} + 0.0531$$

FTIR Spectra of Rifaximin

The FTIR spectrum of Rifaximin confirmed the presence of its characteristic functional groups, indicating structural stability and purity. A broad absorption band at 3402.86 cm⁻¹ corresponds to O-H stretching, signifying hydrogen-bonded hydroxyl groups. Peaks at 3075.15 cm⁻¹ indicate aromatic C-H stretching, while absorptions at 2928.59 and 2863.56 cm⁻¹ represent aliphatic C-H stretching. A sharp peak at 1664.15 cm⁻¹ confirms the C=O stretching of ketone and lactone groups, crucial for the drug's antibacterial activity. Additionally, the C-O-C stretch observed at 1050.42 cm⁻¹ suggests the presence of ether, ester, and lactone functionalities. The absence of unexpected peaks or significant shifts supports the chemical integrity and compatibility of Rifaximin. (Figure 3)

DSC Thermogram of Rifaximin

The DSC of the Rifaximin was carried out by using instrument. The peak of Rifaximin was observed on the 202.08°C which is in the standard range of 200–205°C which confirms the presence of Rifaximin. (Figure 4)

Design and Optimization of RFN-EC-SLN using QbD-based BBD Approach

Thirteen RFN-EC-SLN formulations (F1–F13) were developed using the solvent injection method and optimized using the BBD under the QbD framework. The study evaluated the influence of 3 independent variables lipid concentration (A), surfactant (B), and enteric polymer (C) on particle size (Y1), entrapment efficiency (Y2), and drug release (Y3).

The lipid content ranged from 50–150 mg, surfactant from 200–600 mg, and enteric polymer (Eudragit L100) from 40–80 mg. The optimization aimed to meet the Quality Target Product Profile (QTPP). Statistical analysis

Table 3: Physico-chemical characterization of RFN-EC-SLN

Formulation	Physicochemical Properties					
	Globule size (nm)	PDI	Zeta potential (mV)	EE (%)	RFN loading (%)	pH
RFN-EC-SLN	154 ± 2.6	0.21 ± 0.03	+17.5 ± 0.04	82.0 ± 1.6	10.2 ± 0.2	6.9 ± 0.2

Table 4: *In-vitro* release of RFN from all developed formulations for 24 hours

S. No.	Formulation code	RFN release after 24 hours	Amount of RFN (µg/mL) release from RFN-EC-SLN after 24 hours
1	F1	84 ± 1.2	420
2	F2	75 ± 1.4	375
3	F3	78 ± 1.6	390
4	F4	87 ± 0.6	435
5	F5	82 ± 1.9	410
6	F6	86 ± 2.4	430
7	F7	75 ± 2.6	375
8	F8	78 ± 2.3	390
9	F9	69 ± 0.7	345
10	F10	72 ± 1.1	360
11	F11	74 ± 1.3	370
12	F12	69 ± 0.9	345
13	F13	76 ± 1.4	380

revealed that variables A (lipid) and C (enteric polymer) significantly influenced all three responses ($p < 0.05$), while surfactant concentration (B) had minimal impact. The regression model demonstrated a good fit, with experimental values aligning well with predicted outcomes.

The derived polynomial equations confirmed lipid concentration as the most influential factor, with the highest positive coefficient values for particle size (+205 nm), EE (+73%), and drug release (+78%). This highlights the lipid phase's critical role in determining nanoparticle characteristics and guiding formulation optimization.

Characterization RFN-EC-SLN Formulation

Particle Size

Particle size analysis provides critical insight into the physical characteristics of the developed nanosystem. The optimized RFN-EC-SLN formulation shows a mean particle size of 154 ± 2.6 nm, indicating nanoscale dispersion ideal for enhancing gastrointestinal absorption.

Table 5: Regression coefficients of different kinetic models applied to the RFN-EC-SLN formulation

Release kinetic models	Formulation RFN-EC-SLN (R^2)
Zero-order	0.989
First-order	0.794
Higuchi	0.889
Hixon-Crowell cube root	0.988
Korsmeyer-Peppas	0.916
n = Release exponent	(n = 1.801)

Table 6: Stability Study Data of RFN-EC-SLN

Parameters	Initial	Accelerated Stability (After 3 Months)
Particle size (nm)	154 ± 2.6	158 ± 4.2
PDI	0.21 ± 0.03	0.24 ± 0.04
Zeta potential (mV)	+17.5 ± 0.04	+17.2 ± 0.08
Phase separation	No	No
Physical appearance	Clear	Clear
pH	6.9 ± 0.2	6.8 ± 0.4
RFN content over the period (%)	10.2 ± 0.2	9.95 ± 0.1

The increased surface area of these nanoparticles supports efficient systemic delivery by promoting faster dissolution and uptake.(Figure 5)

Polydispersity Index (PDI)

The Polydispersity Index (PDI) was found to be 0.21 ± 0.03 , suggesting a narrow and uniform size distribution of the nanoparticles. A lower PDI value reflects a homogeneous population of nanoglobules, which is essential for minimizing the risk of aggregation and ensuring formulation stability.

Zeta Potential

The zeta potential was measured at $+17.5 \pm 0.04$ mV for optimized formulation. This positive surface charge can be recognized to the presence of cationic components such as Eudragit L100. (Figure 6)

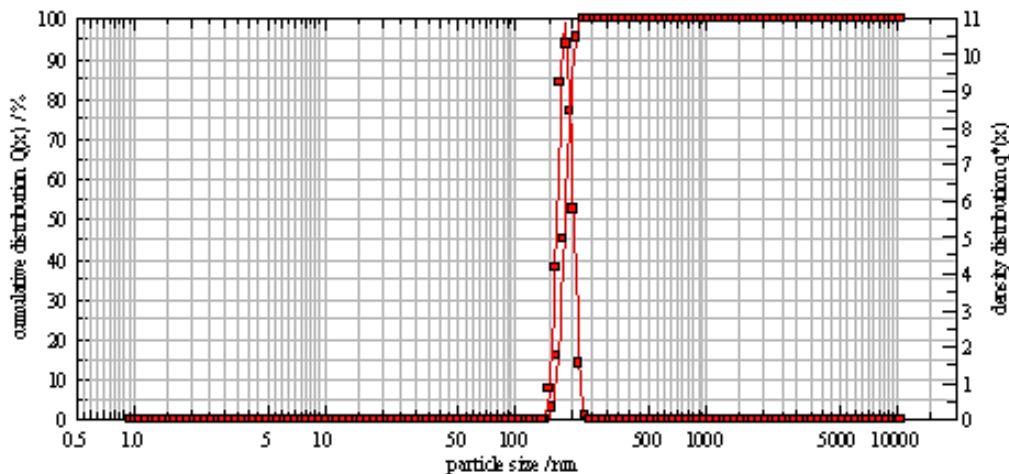


Figure 5: Particle size of optimized RFN-EC-SLN formulation

Entrapment Efficiency (EE %)

The EE% and drug content of the RFN-EC-SLN formulation were assessed to determine the formulation's drug-loading capacity. The formulation exhibited an entrapment efficiency of $82.0 \pm 1.6\%$, indicating successful incorporation of rifaximin within the solid lipid nanoparticle matrix. The drug loading was found to be $10.2 \pm 0.2\%$, confirming the nanosystem's potential as an effective delivery carrier.

Drug Content

These values suggest that the selected formulation components including the lipid matrix, polymer coating, and surfactant system were well-suited for efficiently encapsulating rifaximin. High entrapment and drug-loading capacities are vital for enhancing oral bioavailability, reducing dosing frequency, and improving therapeutic outcomes.

pH Analysis

The pH of the RFN-EC-SLN formulation was determined to be 6.9 ± 0.2 , falling within the acceptable range for oral pharmaceutical preparations (pH 2–9). This pH value closely aligns with the physiological pH of the oral cavity (typically between 6.2 and 7.6), indicating that the formulation is unlikely to cause mucosal irritation or discomfort upon oral administration.

Maintaining a physiologically compatible pH is essential for patient compliance and safety, as it supports the

stability and acceptability of the formulation during transit through the gastrointestinal tract.

Surface Morphology by SEM & TEM

The morphology of the RFN-EC-SLN was examined using SEM, which was discovered to have spherical shape nanoparticles. Particle diameter was determined to be compatible with particle size measurements, and no particle aggregation was seen in the SEM pictures. Additionally, SEM examination demonstrated a homogeneous distribution of spherical particles, which aligned with the microscopy study.

The TEM imaging method was used to examine the internal diameter and morphology of the developed RFN-EC-SLN. It was discovered to be spherical in shape and had a 160 nm diameter. Given that both methods support and validate the nanoscale size of the RFN-EC-SLN particles, the results demonstrated a strong correlation between the DLS and TEM data. As a result, TEM measurements confirm that the nanosystem is distributed uniformly. (Figure 7)

In-vitro Drug Release Studies

Among total 13 formulations, formulation F6 was identified as the most promising based on optimization criteria suggested by the Box–Behnken Design (BBD) and design expert analysis. The release profile of RFN from the optimized RFN-EC-SLN formulation (F6) was assessed using dialysis cassettes with a M.W. cut-off of 2,000 Da. In simulated gastric fluid (pH 1.2), the

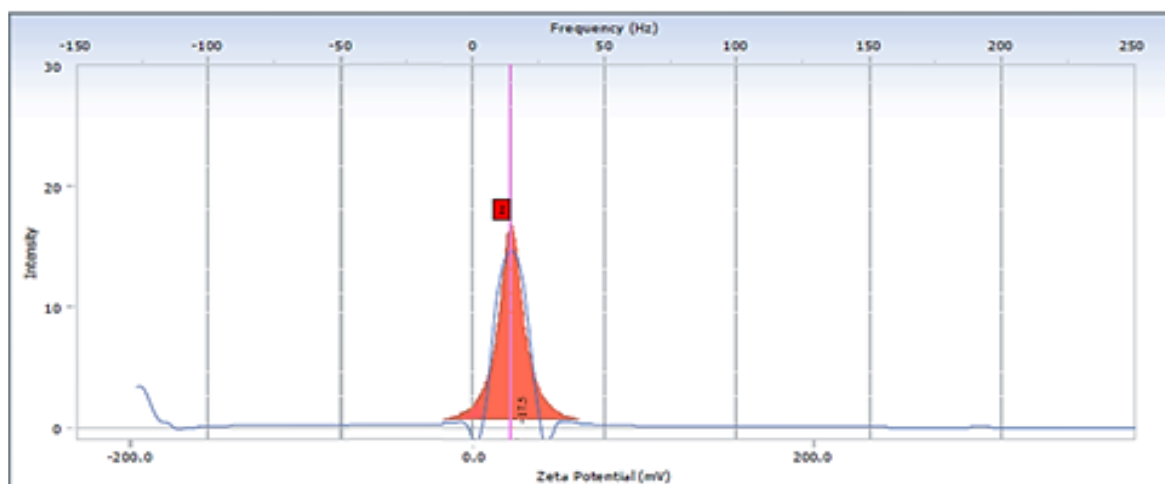


Figure 6: Zeta potential of RFN-EC-SLN Formulation

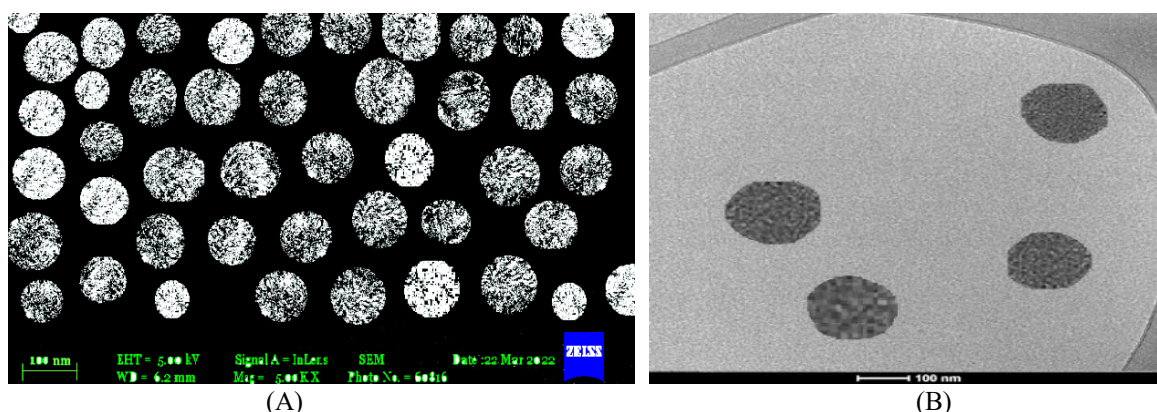


Figure 7: Surface morphology examination of RFN-EC-SLN by (A) SEM and (B) TEM

formulation exhibited a limited release of $15.8 \pm 3.4\%$ RFN over the initial 2 hours, demonstrating gastric resistance. When transitioned to simulated intestinal fluid (pH 6.8), a sustained release pattern was observed, with cumulative RFN release reaching $86.0 \pm 2.4\%$ over 24 hours.

Regression analysis indicated a strong correlation with the zero-order kinetic model ($R^2 = 0.989$), suggesting that the release was concentration-independent and primarily governed by a diffusion-controlled mechanism. Compared to a standard RFN suspension, the SLN formulation exhibited significantly sustained and controlled drug release over the 24-hour period ($*p < 0.05$), confirming its potential for prolonged therapeutic action.

Stability Studies

The optimized RFN-EC-SLN formulation was subjected to accelerated stability testing in compliance with ICH recommendations. Throughout the three-month evaluation, critical parameters remained consistent and within the permissible range. No evidence of instability, including phase separation or visible changes, was detected. The drug content showed negligible variation, with RFN loading maintained at $9.95 \pm 0.1\%$ ($79.6 \pm 2.9\%$) compared to the initial $10.2 \pm 0.2\%$ ($82.0 \pm 1.6\%$). These results confirm that the developed formulation possesses robust physical and chemical stability under accelerated storage conditions.

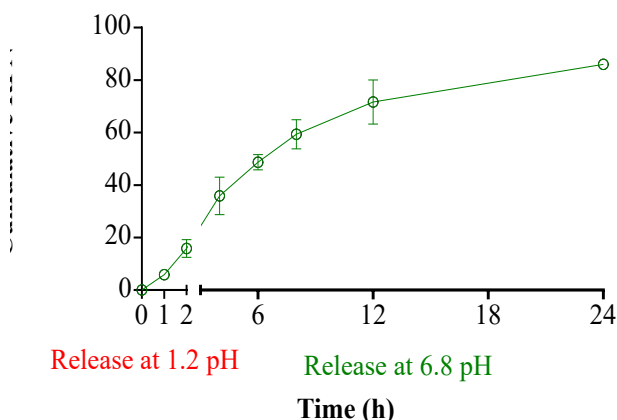


Figure 8: Cumulative RFN release from RFN-EC-SLN over 24 hours via a dialysis cassette

CONCLUSION

The study successfully developed and optimized rifaximin-loaded SLN (RFN-EC-SLN) using a BBD and QbD approach to enhance oral bioavailability, permeability, and stability for the effective treatment of gastrointestinal infections like *Escherichia coli*-induced traveler's diarrhea. The optimized formulation incorporated GRAS-listed, biodegradable excipients including glyceryl monostearate (lipid), Pluronic F68 (surfactant), and Eudragit L100 (polymer), resulting in a stable, non-invasive oral delivery system. The RFN-EC-SLN demonstrated favorable particle size (~ 154 nm), low polydispersity, stable zeta potential, and no phase

separation during accelerated stability studies. It showed sustained in-vitro drug release over 24 hours, improved intestinal permeability, and resistance to enzymatic degradation and first-pass metabolism. Furthermore, the presence of surfactants and polymers aided in inhibiting P-glycoprotein-mediated efflux, enhancing intestinal absorption. Overall, RFN-EC-SLN presents a promising, safe, and effective nanocarrier platform for oral delivery of rifaximin in the management of chronic gastrointestinal complaints, with potential for reduced frequency of dose and minimized side effects.

REFERENCES

- Jain AK, Das M, Swarnakar NK, Jain S. Engineered nanoparticles for oral delivery of poorly soluble drugs: challenges and strategies. *Expert Opin Drug Deliv.* 2011;8(6):753-766. doi:10.1517/17425247.2011.565743.
- Ensign LM, Cone R, Hanes J. Oral drug delivery with polymeric nanoparticles: the gastrointestinal mucus barriers. *Adv Drug Deliv Rev.* 2012;64(6):557-570. doi:10.1016/j.addr.2011.12.009.
- Mercuri A, Passerini N, Hadrich G. Enteric-coated nanoparticles for oral delivery of lipophilic drugs: challenges and opportunities. *Drug Discov Today.* 2022;27(1):218-234. doi:10.1016/j.drudis.2021.09.003.
- Mohanpuria P, Rana NK, Yadav SK. Biosynthesis of nanoparticles: Technological concepts and future applications. *Journal of Nanoparticle Research.* 2008;10(3):507-517.
- Hua S. Advances in oral drug delivery for regional targeting in the gastrointestinal tract: influence of physiological, pathophysiological, and pharmaceutical factors. *Front Pharmacol.* 2020;11:524. doi:10.3389/fphar.2020.00524.
- Sastry SV, Nyshadham JR, Fix JA. Recent technological advances in oral drug delivery: a review. *Pharm Sci Technol Today.* 2019;3(4):138-145. doi:10.1016/S1461-5347(00)00247-9.
- Date AA, Hanes J, Ensign LM. Nanoparticles for oral delivery: design, evaluation, and state-of-the-art. *J Control Release.* 2016;240:504-526. doi:10.1016/j.jconrel.2016.06.016.
- Vivero-Escoto JL, Slowing II, Trewyn BG, Lin VS. Mesoporous silica nanoparticles for intracellular controlled drug delivery. *Small.* 2010;6(18):1952-1967.
- Mittal G, Sahana DK, Bhardwaj V, Ravi Kumar MNV. Enteric-coated nanoparticles for oral drug delivery. In: *Nanoparticulate Drug Delivery Systems*. New York: Informa Healthcare; 2012. p. 135-158.
- Peer D, Karp JM, Hong S, Farokhzad OC, Margalit R, Langer R. Nanocarriers as an emerging platform for cancer therapy. *Nature Nanotechnology.* 2007;2(12):751-760.
- Zhang L, Wang S, Zhang M, Sun J. Nanoparticle-based oral drug delivery systems for poorly soluble drugs: design, optimization, and in-vivo evaluation. *Int J*

- Pharm.* 2020;587:119669.
doi:10.1016/j.ijpharm.2020.119669.
12. Patel V, Agrawal YK, Saraf S. Enteric-coated nanoparticles for targeted oral delivery of a poorly water-soluble drug: formulation and pharmacokinetic assessment. *Drug Deliv Transl Res.* 2019;9(4):789-801. doi:10.1007/s13346-019-00632-3.
 13. Garg NK, Singh B, Jain A, Sharma R. Development and optimization of enteric-coated nanoparticles for enhanced oral bioavailability of a BCS Class II drug. *J Nanopart Res.* 2018;20:156. doi:10.1007/s11051-018-4257-8.
 14. Yadav D, Kumar N. Formulation and characterization of enteric-coated polymeric nanoparticles for pH-sensitive delivery of a poorly soluble anticancer drug. *AAPS PharmSciTech.* 2017;18(6):2187-2196. doi:10.1208/s12249-016-0696-7.
 15. Singh A, Bajpai M. Optimization of Eudragit-based enteric nanoparticles for colon-targeted delivery of a hydrophobic drug using Box-Behnken design. *Drug Dev Ind Pharm.* 2016;42(8):1316-1327. doi:10.3109/03639045.2015.1135939.
 16. Khan S, Batchelor H, Hanson P, Perrie Y, Mohammed AR. Enteric-coated nanoparticles for the oral delivery of poorly soluble drugs: formulation and in vitro evaluation. *Eur J Pharm Sci.* 2021;159:105715. doi:10.1016/j.ejps.2021.105715.
 17. Liu Y, Wang Y, Yang J, Zhang H, Gan L. pH-sensitive polymeric nanoparticles for improved oral delivery of a poorly water-soluble drug: design, optimization, and in vivo pharmacokinetics. *Int J Nanomedicine.* 2020;15:5789-5802. doi:10.2147/IJN.S259525.
 18. Sharma G, Thakur K, Raza K, Singh B. Enteric-coated chitosan-based nanoparticles for colon-targeted delivery of cyclosporine A: formulation, optimization, and in vivo evaluation. *J Microencapsul.* 2019;36(3):234-246. doi:10.1080/02652048.2019.1622599.
 19. Gonçalves LMD, Maestrelli F, Mura P, Cirri M. Development of solid lipid nanoparticles and enteric-coated nanoparticles for oral delivery of a poorly soluble drug: comparative study. *Pharm Dev Technol.* 2018;23(7):718-726. doi:10.1080/10837450.2017.1362433.
 20. Alai MS, Lin WJ, Pingale SS. Application of polymeric nanoparticles and micelles in the delivery of poorly soluble drugs: a review. *J Nanosci Nanotechnol.* 2017;17(4):2304-2317. doi:10.1166/jnn.2017.12825.
 21. Beloqui A, Coco R, Alhouayek M, Solinís MÁ, Rodríguez-Gascón A, Muccioli GG. Budesonide-loaded nanoparticles with pH-sensitive coating for improved mucosal drug delivery in ulcerative colitis. *Nanomedicine.* 2016;11(6):616-628. doi:10.2217/nnm.15.218.
 22. Zhang X, Wu W. Ligand-mediated active targeting for enhanced oral absorption of poorly soluble drugs. *Adv Drug Deliv Rev.* 2015;95:104-115. doi:10.1016/j.addr.2015.09.004.